Supplementary Material for "Quantum reactive scattering of ultracold NH($X\,^3\Sigma^-$) radicals in a magnetic trap"

by Liesbeth M. C. Janssen, Ad van der Avoird, and Gerrit C. Groenenboom

Radboud University Nijmegen, Institute for Molecules and Materials,

Heyendaalseweg 135, 6525 AJ Nijmegen, The Netherlands

QUANTUM REACTIVE SCATTERING METHOD

In this section, we outline the quantum scattering algorithm used to calculate the total NH + NH reactive cross sections. Before discussing our approach in detail, let us recall the basics of already established single-arrangement reactive scattering methods. Conventional single-arrangement algorithms combine a standard inelastic scattering calculation, e.g., renormalized Numerov or log-derivative propagation [1], with complex "capture" reactive boundary conditions. These boundary conditions allow collision flux to disappear into reactive channels at a sufficiently small value of the radial coordinate R. The corresponding solutions to the coupled-channels equations become complex-valued and, as a consequence, the scattering S-matrix is no longer unitary. The deviation from unitarity is then used to extract the reactive collision cross sections [2, 3]. Here we employ a different strategy and first calculate, for a given interval $[R_0, R_n]$, two sets of *real-valued* solutions to the coupled-channels equations. This is most conveniently done using the renormalized Numerov propagation algorithm [1]. The "regular" solutions F satisfy $F(R_0) = 0$ and $F(R_n) = 1$, and the "irregular" solutions G are defined by $G(R_0) = 1$ and $G(R_n) = 0$. A suitable linear combination of these functions, determined by the scattering boundary conditions, provides the final scattering wave function. We note that the irregular functions are equivalent to the *regular* solutions on the *reversed* radial grid, i.e. the regular solutions obtained by propagating from R_n to R_0. It is, however, also possible to obtain both sets of solutions in a single propagation run, as detailed in Ref. [4].

The regular and irregular functions form a *complete* set of linearly independent solutions for a given energy E. Hence, once the propagation is completed, we may enforce all possible boundary conditions to construct all possible scattering wave functions for a given Hamiltonian and energy. This represents a major advantage over conventional reactive scattering (log-derivative propagation) methods, for which the boundary conditions must be imposed at the start of the propagation [2, 3]. The fact that the boundary conditions can be applied *after* our propagation routine also implies that the scattering code can be parallelized to speed up the calculation. Such a parallelization may be realized by solving the coupled-channels equations

for different radial intervals, e.g. for $[R_0, R_1]$, $[R_1, R_2]$,..., and $[R_{n-1}, R_n]$, and matching the solutions afterwards on the interval $[R_0, R_n]$.

The scattering S-matrix can be obtained by matching the numerical solutions for $[R_0, R_n]$ to the analytical solutions for $R < R_0$ and $R > R_n$. This S-matrix contains both reactive and non-reactive blocks, collectively forming a *unitary* matrix (provided that the total flux is conserved and the radial grid is converged). We have applied reactive scattering boundary conditions with incoming flux in the asymptotic NH + NH channels, and outgoing flux both in asymptotic (non-reactive) channels and in reactive NHNH channels near the origin ($R_0 = 4.5\ a_0$). In the asymptotic region, we matched the incoming and outgoing waves to the usual spherical Bessel functions. In the short range, we took the local adiabatic eigenvalues as reactive channel energies and matched to Airy functions. The slope of the adiabats was used to distinguish between open and closed reactive channels (see also Refs. [3, 4]). Note that our boundary conditions allow for reflection not only off the quintet potential, but also off the reactive singlet and triplet potentials. Such a situation can occur if the local adiabats are dominated by repulsive orientations.

The scattering calculations for NH + NH collisions in an external magnetic field were performed in the uncoupled channel basis set defined in Ref. [5]. The basis was truncated at a monomer rotational angular momentum of $N_{\max} = 2$ and a partial-wave angular momentum of $L_{\max} = 6$. We considered only channel functions with even permutation symmetry and even parity, and a space-fixed total angular momentum projection of $\mathcal{M} = 2$. As outlined in Ref. [5], this basis set allows for collisions with even partial waves (e.g. s-waves) between identical bosonic molecules in the same initial quantum state. Since the ultracold regime is s-wave dominated, the $\mathcal{M} = 2$ cross sections are the most relevant at the energies considered in this work.

It has already been established in previous non-reactive scattering studies that our channel basis set, truncated at $N_{\max} = 2$, is insufficiently large to ensure convergence of the cross sections [5–7]. However, it was also shown that full convergence is not strictly necessary to obtain useful insight into the collision dynamics [5, 6]. In order to clarify this statement, let us first consider the effects of small uncertainties in the potentials (see Fig. 5 of the main article). The presence of (quasi-)bound states in the NH–NH system gives rise to scattering resonances which can alter the collision cross sections by several orders of magnitude. Since the exact forms of the potentials, and thus the exact locations of the resonances, are unknown, the cross sections are subject to an inherent degree of uncertainty. Nevertheless, by means of λ-scaling, one can still provide a reliable estimate of the *likelihood* that evaporative cooling will proceed. The same holds for, e.g., the relative importance of the various collisional mechanisms involved, which can be established without knowing the precise shape of the potentials. It was shown for the non-reactive scattering case that these qualitative results and conclusions are fairly independent of the channel basis set size. More

specifically, the effect of using a reduced basis set was found to be very similar to a scaling of the potential within its uncertainty [5, 6]. Hence, even without obtaining full basis set convergence, one can obtain a realistic qualitative picture of the collision dynamics. A recent study by Suleimanov *et al.* on non-reactive scattering of magnetically trapped NH radicals using a fully converged basis set supports these findings [7].

In the present work, we extend the λ-scaling approach and the effect of basis set size to the *reactive* scattering case. We have performed additional reactive scattering calculations as a function of λ for a larger basis, truncated at $N_{\max} = 3$, for a collision energy of 10^{-6} K and a magnetic field strength of 1 G. The results are shown in Fig. S1. The data for $N_{\max} = 2$ (Fig. 5 of the main article) are also plotted for comparison. It can be seen that the use of a larger basis set leads to a shift of the resonance peaks in both the reactive and non-reactive cross sections, but the qualitative pattern remains almost unaltered. The same result was found earlier for the non-reactive NH + NH scattering case [5, 6].

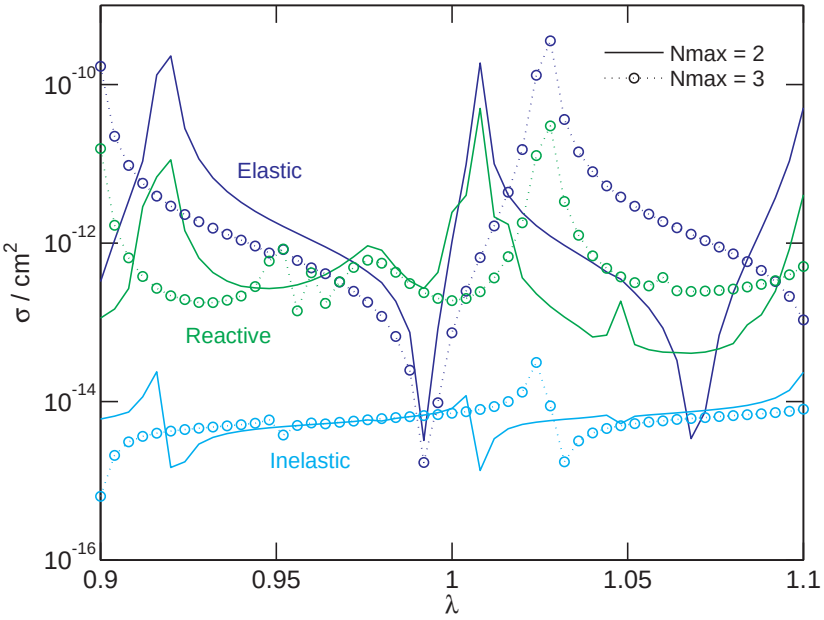

FIG. S1: Elastic, inelastic, and reactive NH + NH collision cross sections for different basis sets as a function of the scaling parameter λ, calculated at a collision energy of 10^{-6} K and a magnetic field strength of 1 G.

It is known from previous work that a fully converged basis set for NH + NH should be truncated at $N_{\max} \geq 6$ [6, 7], and the results shown in Fig. S1 are therefore still far from convergence. Due to limitations in computer power, we consider it infeasible at present to perform scattering calculations for $N_{\max} > 3$ in the uncoupled channel basis set. The computational cost is significantly reduced, however, by employing a total angular momentum representation [6, 7]. We have carried out additional calculations up to $N_{\max} = 6$ using the coupled total angular momentum basis set of Ref. [6], and assuming zero magnetic

field. Since the reactive cross sections are quite insensitive to the magnetic field strength, we expect this to be a reasonable assumption. That is, the field-free results should be an accurate reflection of the true reactive scattering data in a nonzero magnetic field. Figure S2 shows the field-free elastic and reactive cross sections as a function of λ for a collision energy of 10^{-6} K. The elastic-to-reactive cross section ratio (γ) is also shown. All calculations were performed with a maximum partial-wave angular momentum of $L_{\max} = 6$; the expansion of the potential energy surfaces was truncated at $L_A = L_B = 6$ (see Eq. 2 of Ref. [8]). It can be seen that the convergence behavior of the reactive cross sections is similar to that of the elastic ones: the resonance features may shift as $N_{\max}$ increases, but the pattern remains approximately the same. In particular, the *likelihood* of finding a particular elastic-to-reactive collision ratio (assuming that $0.9 \leq \lambda \leq 1.1$ adequately samples the range of possibilities for the true potentials) is fairly independent of $N_{\max}$. Consequently, we can reliably predict the feasibility of evaporative cooling of NH based on the data obtained with an incompletely converged basis set. The same argument applies to, e.g., the prospects for magnetic field control of NH + NH chemistry. Thus, even without obtaining full basis set convergence, we can provide useful insight into the reactive scattering dynamics of the NH + NH system. This is completely analogous to the non-reactive scattering case investigated earlier [5–7].

QUANTUM-DEFECT MODEL

In order to establish the degree of universality for cold and ultracold NH + NH reactions (see Figs. 4 and 5 of the main article), we have employed the single-channel quantum-defect model of Idziaszek and Julienne [9]. This model parameterizes the collision dynamics in terms of two dimensionless parameters, s and y, which represent a reduced scattering length and short-range reaction probability, respectively. In the universal limit, y is unity and all scattering flux that reaches the short range disappears into (exoergic) reactive channels. The role of the long-range potential is to determine how much of the entrance-channel wave is transmitted to the short range to experience such reactive "loss" dynamics. For a single isotropic potential, the universal elastic and reactive cross sections for s-wave collisions are given by [9]

$$\sigma_{\text{elastic}}(k) = 4g\bar{a}^2, \tag{1}$$

$$\sigma_{\text{reactive}}(k) = 2g\frac{\bar{a}}{k}, \tag{2}$$

where k is the wavenumber for the entrance channel and $g = 2$ is a symmetry factor accounting for the identical-particle symmetry. This symmetry factor has also been included in the numerical coupled-channels calculations. The parameter $\bar{a}$ denotes the mean scattering length; it is related to the van der Waals radius $R_6 = \frac{1}{2}(2\mu C_6/\hbar^2)^{1/4}$ as $\bar{a} = 4\pi R_6/\Gamma(1/4)^2$, with Γ being the Gamma function (see also Ref. [10]).

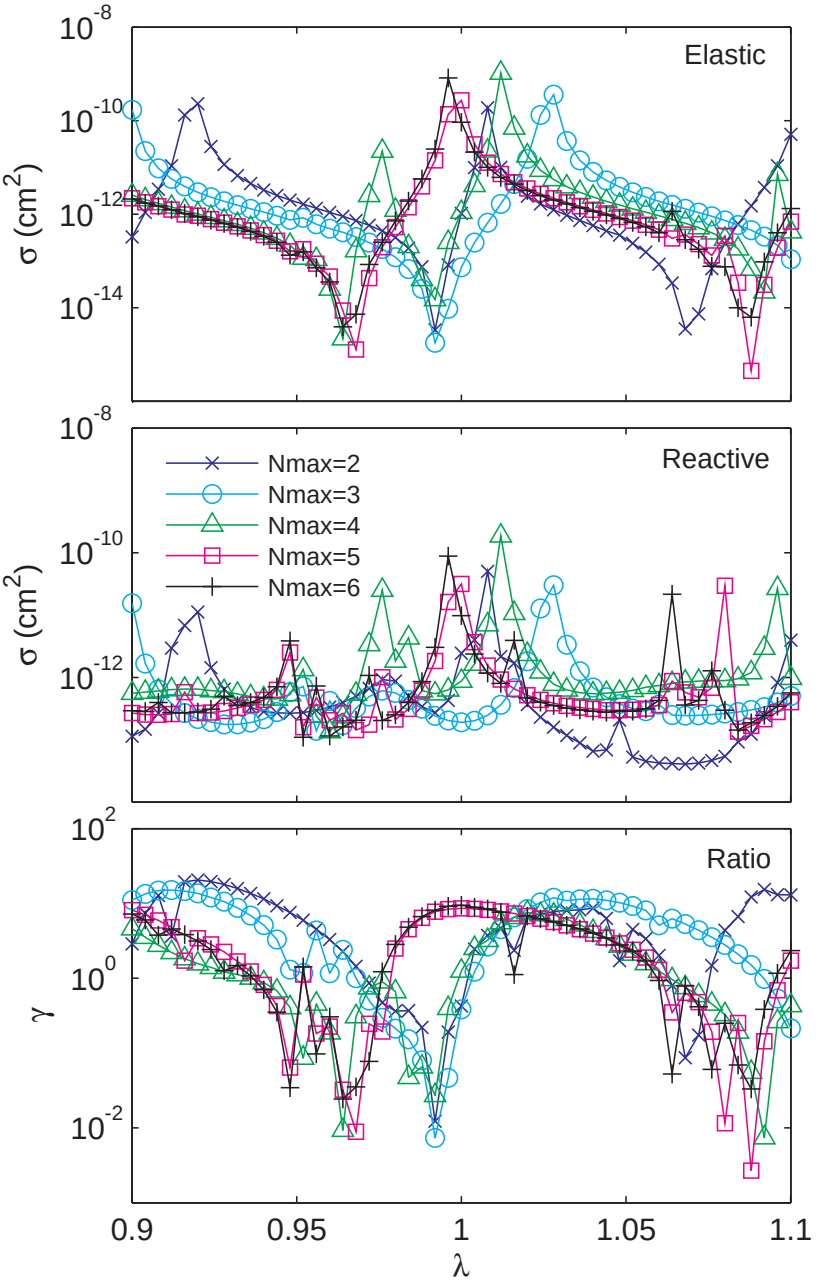

FIG. S2: Elastic (top panel) and reactive (middle panel) NH + NH collision cross sections as a function of the scaling parameter λ, calculated for different basis sets at a collision energy of 10^{-6} K. The magnetic field was set to zero. The bottom panel shows the ratio between the elastic and reactive cross sections.

For the isotropic C_6 coefficient of NH + NH, we take the fitted electronic second-order (dispersion/induction) coefficient calculated in Ref. [8], $C_6^{\rm elec} = 47.27$ a.u., plus a term arising from the mixing of rotational states due to the electric dipole-dipole interaction [4]. The latter is given by $C_6^{\rm dip-dip} = \frac{1}{3}\mu_1^2\mu_2^2/(B_1 + B_2)$, where μ_i and B_i denote the permanent electric dipole moment and rotational constant

of molecule i, respectively. For ^{15}NH + ^{15}NH, we have $\mu_1 = \mu_2 = 1.52$ D and $B_1 = B_2 = 16.270$ cm^{-1}, yielding a total isotropic C_6 coefficient of $C_6^{\mathrm{elec}} + C_6^{\mathrm{dip-dip}} = 338.45$ a.u.

[1] B. R. Johnson, NRCC Proceedings **5**, 86 (1979).

[2] G. C. Groenenboom and L. M. C. Janssen, in *Tutorials in molecular reaction dynamics*, edited by M. Brouard and C. Vallance (RSC, Cambridge, 2010).

[3] E. J. Rackham, T. Gonzalez-Lezana, and D. E. Manolopoulos, J. Chem. Phys. **119**, 12895 (2003).

[4] L. M. C. Janssen, Ph.D. thesis, Radboud University Nijmegen (2012), available online at http://www.theochem.ru.nl/files/theses/janssen-phdthesis-2012.pdf.

[5] L. M. C. Janssen, P. S. Żuchowski, A. van der Avoird, G. C. Groenenboom, and J. M. Hutson, Phys. Rev. A **83**, 022713 (2011).

[6] L. M. C. Janssen, P. S. Żuchowski, A. van der Avoird, J. M. Hutson, and G. C. Groenenboom, J. Chem. Phys. **134**, 124309 (2011).

[7] Y. V. Suleimanov, T. V. Tscherbul, and R. V. Krems, J. Chem. Phys. **137**, 024103 (2012).

[8] L. M. C. Janssen, G. C. Groenenboom, A. van der Avoird, P. S. Żuchowski, and R. Podeszwa, J. Chem. Phys. **131**, 224314 (2009).

[9] Z. Idziaszek and P. S. Julienne, Phys. Rev. Lett. **104**, 113202 (2010).

[10] G. F. Gribakin and V. V. Flambaum, Phys. Rev. A **48**, 546 (1993).